Heliyon 10 (2024) e32800

Contents lists available at ScienceDirect

Heliyon

journal homepage: www.cell.com/heliyon

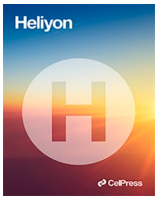

Research article

NIR-II light therapy improves cognitive performance in MPTP induced Parkinson's disease rat models: A preliminary experimental study

Jiangong Zhang [a,1], Qinqin Zhu [b,1], Xun Shi [a,1], Yang Huang [c], Linlin Yan [b], Guozheng Zhang [b], Lei Pei [b], Jiahuan Liu [b], Xiaowei Han [b,*,1], Xisong Zhu [b,**,1]

[a] *Department of Nuclear Medicine, The First People's Hospital of Yancheng, Yancheng First Hospital, Affiliated Hospital of Nanjing University Medical School, The First Affiliated Hospital of Jiangsu Vocational College of Medicine, Yancheng, Jiangsu, China*
[b] *Department of Radiology, The Quzhou Affiliated Hospital of Wenzhou Medical University, Quzhou People's Hospital, Quzhou, China*
[c] *The Second School of Clinical Medicine, Zhejiang Chinese Medical University, Hangzhou, China*

A R T I C L E I N F O

Keywords:
MPTP
Parkinson's disease
Behavior analysis
Cognitive impairment
Multiplex immunohistochemistry

A B S T R A C T

Cognitive impairment is an important component of non motor symptoms in Parkinson's disease (PD), and if not addressed in a timely manner, it can easily progress to dementia. However, no effective method currently exists to completely prevent or reverse cognitive impairment associated with PD. We therefore aimed to investigate the therapeutic effect of near-infrared region II light (NIR-II) region illumination on cognitive impairment in PD through behavioral experiments (water maze and rotary rod) and multiple fluorescence immunohistochemistry techniques. The 1-methyl-4-phenyl-1, 2, 3, 6-tetrahydropyridine (MPTP)-induced group was compared with the MPTP- untreated rat group, showing a significant reduction in escape latency and significant increase in the fall latency in the MPTP-treated group. The horizontal analysis results indicated that NIR-II phototherapy improved the learning and cognitive abilities as well as coordination and balance abilities of rats. Post-treatment, the MPTP rats showed significantly shortened, escape latency, prolonged target quadrant residence time, and prolonged fall latency compared with pre-treatment. The longitudinal analysis results reaffirmed that NIR-II phototherapy improved the learning and cognitive abilities as well as coordination and balance abilities of rats. The multiple fluorescence immunohistochemistry analysis trend plot showed that the activated microglia and astrocytes in the hippocampus were highest in MPTP-induced PD untreated group, moderate in MPTP-induced PD treatment group, and lowest in the control group. Our data indicates that NIR-II illumination improves learning and cognitive impairment as well as coordination and balance abilities in PD rats by downregulating the activation of microglia and astrocytes in the hippocampus.

* Corresponding author. Department of Radiology, The Quzhou Affiliated Hospital of Wenzhou Medical University, Quzhou People's Hospital, Quzhou, China.
** Corresponding author.
E-mail addresses: hxw2002hxw@163.com (X. Han), zhuxisong@126.com (X. Zhu).
[1] These authors have contributed equally to this work.

https://doi.org/10.1016/j.heliyon.2024.e32800
Received 10 December 2023; Received in revised form 7 June 2024; Accepted 10 June 2024
Available online 11 June 2024
2405-8440/© 2024 Published by Elsevier Ltd. This is an open access article under the CC BY-NC-ND license (http://creativecommons.org/licenses/by-nc-nd/4.0/).

1. Introduction

Parkinson's disease (PD) is a progressive degenerative disease of the central nervous system, with a predilection age 50–65 years old. Typical pathological changes include degeneration and death of dopaminergic neurons in the substantia nigra pars compacta, leading to motor disorders such as static tremors and postural gait instability. PD is accompanied by a series of non-motor symptoms, including cognitive impairment and autonomic nerve damage [1]. PD with cognitive impairment (PD-CI) is characterized by delayed cognitive speed, impaired abstract thinking, and memory difficulties. PD-CI is further divided into PD with mild cognitive impairment (PD-MCI) and PD with dementia (PDD). If PD-CI is not treated promptly, the risk of PD-MCI converting into PDD increases [2,3]. PDD seriously affects the patients' daily lives and reduces their quality of life. Currently, most studies have focused on the decline in motor ability caused by PD; however, improving cognitive impairment is also an urgent issue that needs to be addressed.

The application of optical related technologies in medicine is becoming increasingly widespread [4,5]. Photobiological modulation (PBM), a noninvasive and effective physical therapy method, is highly promising for treating brain dysfunction. PBM involves the application of light-emitting diodes or lasers of specific wavelengths to stimulate the body, causing biochemical reactions or functioning within tissue cells. The theoretical basis is that biological tissues absorb light energy and convert it to chemical or thermal energy, leading to a series of chemical reactions in the body. PBM alleviates pain, reduces inflammation, and promotes the repair of damaged cells and tissues [6,7]. It does not need to reach specific areas through the blood circulation to function and can directly act on the treatment site, which differs from traditional drug therapy. The intensity, wavelength, frequency, and duration of light affect the effectiveness of treatment [8–11]. PBM has been widely used in neurodegenerative diseases, such as PD, and has achieved good therapeutic effects [12–16]. Transcranial PBM is currently the most commonly used treatment method, mostly using red-to-near-infrared range light (600–1100 nm). Owing to the obstruction of cranial tissues (including the scalp, soft tissue, periosteum, skull, and meninges), the amount of light energy decreases exponentially, and the energy ultimately reaching the brain parenchyma is very limited. Therefore, although this method is safe and noninvasive, its efficiency is low. Compared with the near-infrared region I (700–900 nm), near-infrared region II light (NIR-II, 1000–1700 nm) has the advantages of longer wavelengths, less scattering, and stronger penetration [17,18].

The compound 1-methyl-4-phenyl-1,2,3,6-tetrahydropyridine (MPTP) is a neurotoxin with strong lipophilicity that can enter the central nervous system through the blood-brain barrier, causing a series of reactions such as oxidative stress, inflammation, and mitochondrial apoptosis, ultimately leading to damage to dopaminergic neurons in the substantia nigra [19,20]. This study aimed to explore the therapeutic effects of NIR-II illumination on cognitive impairment in MPTP-induced PD rats using behavioral experiments and multiple fluorescence immunohistochemistry techniques.

2. Materials and methods

2.1. Experimental animals

We used 23 pathogen-free male Sprague-Dawley rats (6 weeks old, weighing approximately 200 g) provided by the Jiangsu Vocational College of Medicine (License No. SYXK2023-0005). At the end of the experiment, rats were euthanized by spinal dislocation.

2.2. Model establishment

2.2.1. Materials

The parameters of the NIR-II treatment box are: external box: 892 × 532 × 359 mm, internal box: 770 × 410 × 214 mm, the average power of the LED array can be adjusted from 100 to 1000mw, the light pulse frequency can be adjusted from 10 to 100Hz, the adjustment accuracy is 10Hz, and the duty cycle is 50 %. The ANY-maze water maze test system was purchased from Stoelting Company, IL, USA. The rota-rod rotator was from Ugo Basile S.R.L., Gemonio, Italy. MPTP was purchased from Shanghai McLean Biochemical Technology Co., Ltd., Shanghai, China (batch number: C15375727).

2.2.2. Animal

Before the experiment, the rotating rod and ANY-Maze water maze were used to detect and screen rats with rotating rods for less than 5 min and those who could not swim. First, all animals were numbered consecutively, and then grouped according to the random number table method. Twenty-three rats were randomly divided into the MPTP (n = 16, numbered 1–16, 30 mg/kg) and control groups(equal volume of normal saline). The MPTP group was administered an intraperitoneal injection of 1.5 ml MPTP(concentration, 5 mg/ml) once daily for 7 days.

2.3. The first water maze test and rotating rod experiment

After MPTP injection, the rats were subjected to a water maze test using the ANY-maze system to assess their spatial learning and memory abilities [21]. The background of the water maze was black, and the circular pool was divided into four quadrants. The inner walls of each quadrant were adorned with white stickers of different shapes as reference materials for recognition and memory. The colorless circular platform was located approximately 1–2 cm below the water surface in the second quadrant. The test included a positioning cruise phase (days 1–4) and a spatial search phase (day 5). During the positioning and cruising phases, each rat underwent

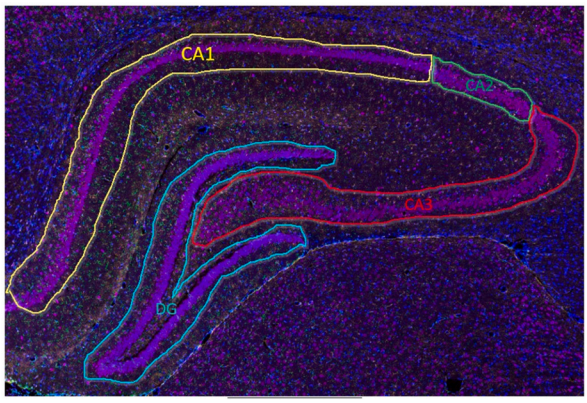

Fig. 1. Schematic diagram of hippocampal subregion delineation.

four training sessions daily, each time entering the water from different quadrants. Each time limit was 60 s, during which the system automatically tracked and calculated the escape latency of the rats reaching the platform using a camera. In the spatial search phase, the platform was removed, rats were introduced to the water from the fourth quadrant (diagonal quadrant of the platform), and the percentage of the rats' residence time in the second quadrant (target quadrant) and the number of times they crossed the platform area within 60 s was recorded and analyzed.

After the water maze test, rats were placed on a rotating rod tester to test their balance [22]. The time limit for the testing process was 300 s. The test mode was the acceleration mode, with a starting speed of 5 rpm and a gradual increase to 10 rpm within 300 s. The drop latency period was the time taken for the rats to persist without falling on the rotating stick instrument, with a maximum of 300 s.

2.4. NIR-II phototherapy

Rats 9–16 in the MPTP group (MPTP-NIR-II) were placed in a specific NIR-II light therapy box for 10 h of light per day for 14 days. The treatment parameters were as follows: irradiation wavelength, 1070 ± 50 nm, irradiation power, 500 mW, and light pulse frequency, 50Hz. The control group did not receive any treatment. During the treatment period, rats could walk, explore, and rest.

2.5. The second water maze test and rotating rod experiment

After MPTP-NIR-II treatment, all rats underwent a second water maze test and a rod rotation experiment.

2.6. Multiple fluorescence immunohistochemistry

After the second behavioral experiment, cold phosphate buffer was infused into the hearts of rats under deep anesthesia, and the brains were used for multiple fluorescence immunohistochemical detection. The scan results were quantitatively analyzed using HALO Highplex FL (Indica Labs; Albuquerque, NM, USA) of the Halo software. Referring to the rat brain atlas (George Paxinos and Charles Watson, 6th edition), the CA1/CA2/CA3/DG subregions of the hippocampus in the HALO system were manually delineated according to the different hippocampal subregions delineated (Fig. 1), the number and size of immune-positive cells were automatically extracted and calculated, and inter-group analyses and comparisons were performed.

2.7. Data processing

Data are expressed as mean ± standard deviation. The escape latency data from the water maze navigation experiment were analyzed using repeated measures analysis of variance(ANOVA). The independent sample *t*-test was used to analyze residence time in the target quadrant, the number of crossing platforms and the drop latency between the two groups (model and control groups) before treatment. The target quadrant residence time, platform crossing times, and drop latency among the three groups (the MPTP -untreated, MPTP -treated, and control groups) were analyzed using one-way ANOVA. The data of platform crossing times and drop latency before and after treatment were analyzed using the paired *t*-test. Descriptive statistical analysis was applied to analyze the results of multicolor fluorescence immunohistochemistry. The statistical significance was set at $P < 0.05$.

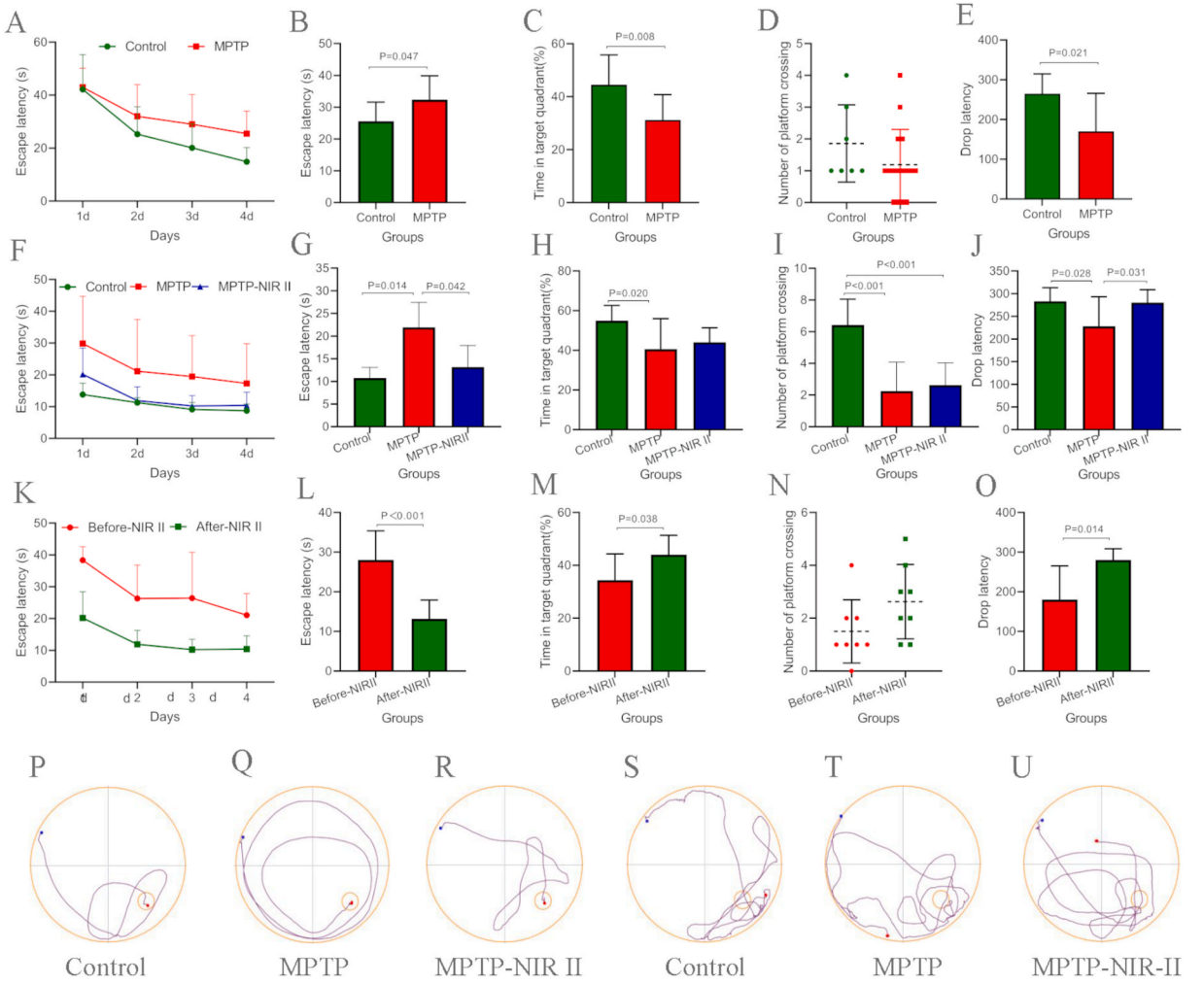

Fig. 2. Panels A and B are the escape latency of control and MPTP groups; Panels C and D are the percentage of residence time in the target quadrant and the number of crossing the platform of the two groups of rats, respectively; Panel E is the drop latency of two groups. Panels F and G are the escape latency of control, MPTP and MPTP-NIR II groups; Panels H and I are the percentage of residence time in the target quadrant and the number of crossing the platform of the three groups of rats, respectively; Panel J is the drop latency of three groups. Panels K and L indicate the escape latency of MPTP group before and after NIR-II treatment; Panels M indicate N are the percentage of residence time in the target quadrant and the number of crossing the platform of MPTP group before and after NIR-II treatment, respectively; Panel O is the drop latency of MPTP group before and after NIR-II treatment. Panels P–R are the positioning cruise trajectory maps of the control, MPTP, and MPTP-NIR II groups; Panels S–U are the space exploration trajectory diagram of the three groups. MPTP, 1-methyl-4-phenyl-1,2,3,6-tetrahydropyridine; NIRII, Near infrared region II.

Table 1
Comparison of escape latency between two groups of rats.

Groups	n	1d	2d	3d	4d	F	P
Control	7	42.17 ± 13.08	25.28 ± 10.37	20.13 ± 9.03	14.85 ± 5.39	4.47	0.047
MPTP	16	42.99 ± 7.20	32.05 ± 11.94	29.01 ± 11.21	25.47 ± 8.52		

MPTP, 1-methyl-4-phenyl-1,2,3,6-tetrahydropyridine.

3. Results

3.1. Lateral analysis of NIR-II illumination efficacy

3.1.1. The effect of MPTP on the biological behavior of rats

Compared with that of the control group, the escape latency of the MPTP group was prolonged (F = 4.47, P = 0.047) (Fig. 2A and B), the residence time in the target quadrant was shortened (t = 2.93, P = 0.008; 95%CI: 3.85–22.77) (Fig. 2C), and the number of

Table 2
Comparison of spatial exploration ability and drop latency between two groups of rats.

Groups	N	Water maze test		Rotary rod test
		Time in target quadrant(%)	Number of platform crossing(count)	Drop latency
Control	7	44.54 ± 11.24	1.86 ± 1.21	265.00 ± 49.94
MPTP	16	31.24 ± 9.51	1.19 ± 1.11	170.25 ± 95.74
t		2.93	1.29	2.49
P		0.008	0.209	0.021

MPTP, 1-methyl-4-phenyl-1,2,3,6-tetrahydropyridine.

Table 3
Comparison of escape latency among three groups of rats.

Groups	n	1d	2d	3d	4d	F	P
Control	7	13.81 ± 3.58	11.28 ± 1.54	9.14 ± 2.16	8.73 ± 2.10	4.11	0.032
MPTP	8	29.84 ± 14.88	21.15 ± 16.28	19.48 ± 12.89	17.33 ± 12.49		
MPTP-NIRII	8	20.20 ± 8.24	11.90 ± 4.39	10.24 ± 3.23	10.39 ± 4.19		

MPTP, 1-methyl-4-phenyl-1,2,3,6-tetrahydropyridine; NIRII, Near infrared region II.

Table 4
Comparison of spatial exploration ability and drop latency among three groups of rats.

Groups	N	Water maze test		Rotary rod test
		Time in target quadrant(%)	Number of platform crossing(count)	Drop latency
Control	7	54.95 ± 7.70	6.43 ± 1.62	283.43 ± 29.77
MPTP	8	40.65 ± 15.31	2.25 ± 1.83	228.23 ± 65.02
MPTP-NIRII	8	44.08 ± 7.31	2.63 ± 1.41	280.38 ± 28.26
F		3.45	14.72	3.72
P		0.049	<0.001	0.042

MPTP, 1-methyl-4-phenyl-1,2,3,6-tetrahydropyridine; NIRII, Near infrared region II.

Table 5
Comparison of escape latency in MPTP rats before and after treatment (n = 8).

Groups	1d	2d	3d	4d	F	P
Before NIR II	38.37 ± 4.25	26.32 ± 10.50	26.43 ± 14.43	21.08 ± 6.76	28.82	<0.001
After NIR II	20.20 ± 8.24	11.90 ± 4.39	10.24 ± 3.23	10.39 ± 4.19		

MPTP, 1-methyl-4-phenyl-1,2,3,6-tetrahydropyridine; NIRII, Near infrared region II.

Table 6
Comparison of spatial exploration ability and drop latency of MPTP rats before and after treatment (n = 8).

Index	Before NIR II	After NIR II	t	P
Time in target quadrant(%)	34.42 ± 9.90	44.08 ± 7.31	2.56	0.038
Number of platform crossing(count)	1.50 ± 1.20	2.63 ± 1.41	1.43	0.19
Drop latency	180.50 ± 84.52	280.38 ± 28.26	3.25	0.014

MPTP, 1-methyl-4-phenyl-1,2,3,6-tetrahydropyridine; NIRII, Near infrared region II.

platform crossings showed a decreasing trend (Fig. 2D). In the rod-rotation experiment, the fall latency of the MPTP group was shorter (t = 2.49, P = 0.021; 95%CI:15.75–173.75) (Fig. 2E) (Tables 1 and 2).

3.1.2. Effects of NIR-II on MPTP rats

The differences in escape latency (Fig. 2P-R), target quadrant residence time, number of crossing platforms(Fig. 2S-U), and drop latency between the three groups of rats were statistically significant (F = 4.11, 4.45, 14.72, and 3.72, respectively; P = 0.032, 0.049, <0.001, and 0.042, respectively). In the water maze experiment, compared with that of the untreated group, the escape latency of the MPTP-NIR-II group was significantly shortened (P = 0.042; 95%CI: 0.36–17.18) (Fig. 2F and G), with an increasing trend in the residence time in the target quadrant and the number of crossing platforms (Fig. 2H and I). In the rod-rotation experiment, the MPTP-NIR-II group showed a significantly prolonged fall latency (P = 0.031; 95%CI : 5.31–99.19) compared with the untreated group (Fig. 2J) (Tables 3 and 4).

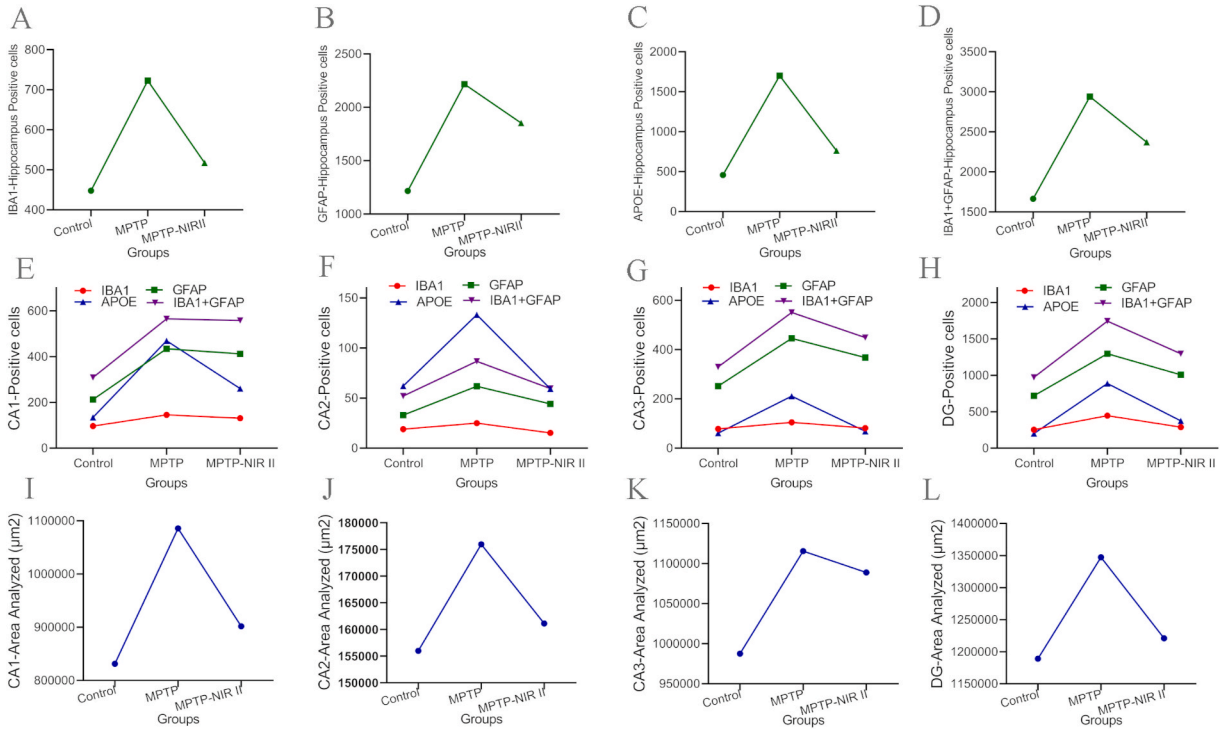

Fig. 3. Panels A–D are the number of IBA1, GFAP, APOE, and IBA1+GFAP positive cells in the hippocampus of the control group, MPTP group, and MPTP-NIR II group, respectively. Panels E–F are the number of IBA1, GFAP, APOE and IBA1+GFAP positive cells in the hippocampal subregion of three groups, respectively. Panels I–L are the area of positive cells in the hippocampal subregion of three groups respectively. MPTP, 1-methyl-4-phenyl-1,2,3,6-tetrahydropyridine; NIRII, Near infrared region II; IBA1, ionised calcium-binding adapter molecule 1; GFAP, glial fibrillary acidic protein; APOE, apolipoprotein E.

Table 7
Analysis of the number of positive cells in the total hippocampus of rats in the three groups(n = 4).

Cells	Control(n = 4)	MPTP(n = 4)	MPTP-NIR II(n = 4)	F	P
$IBA1^+$ Cells	447.75 ± 171.69	722.75 ± 240.17	517.50 ± 154.52	2.21	0.166
$GFAP^+$ Cells	1216.25 ± 589.66	2216.50 ± 1022.64	1852.75 ± 1381.58	0.93	0.429
$APOE^+$ Cells	457.25 ± 260.04	1701.50 ± 2346.79	762.00 ± 451.58	0.87	0.450
$IBA1^+GFAP$	1664.00 ± 648.17	2939.25 ± 1214.85	2370.25 ± 1480.96	1.20	0.346

MPTP, 1-methyl-4-phenyl-1,2,3,6-tetrahydropyridine; NIRII, Near infrared region II; IBA1, ionised calcium-binding adapter molecule 1; GFAP, glial fibrillary acidic protein; APOE, apolipoprotein E.

3.2. Longitudinal analysis of NIR-II illumination efficacy

Compared with before treatment, the escape latency of MPTP rats after treatment was significantly shortened ($F = 28.92$, $P < 0.001$) (Fig. 2K-L), the target quadrant residence time was significantly prolonged ($t = 2.56$, $P = 0.038$; 95%CI : 0.74–18.59) (Fig. 2M), and the number of crossing platforms showed an increasing trend (Fig. 2N). Additionally, in the rod-rotation experiment, the fall latency of MPTP rats was significantly prolonged after treatment ($t = 3.25$, $P = 0.014$; 95%CI : 27.17–172.58) (Fig. 2O) (Tables 5 and 6).

3.3. Multiple immunofluorescence histochemistry

3.3.1. Analysis of absolute expression of positive cells in the hippocampus

On the trend chart, the absolute values of ionised calcium-binding adapter molecule 1- (IBA1), glial fibrillary acidic protein-(GFAP), and apolipoprotein E (APOE)-positive cells were highest in the MPTP-untreated group, intermediate in the MPTP-NIR-II group, and lowest in the control group (Fig. 3A–D, Table 7).

3.3.2. Absolute value analysis of positive cells in each hippocampal subregion

On the trend chart, the absolute values of IBA1-, GFAP-, APOE-, and IBA1+GFAP-positive cells in each subregion were highest in

Table 8
Analysis of positive cell count in the hippocampal subregion of three groups of rats.

Subregions	Groups	IBA1$^+$ Cells	GFAP$^+$ Cells	APOE$^+$ Cells	IBA1$^+$GFAP Cell
CA1	Control	96.25 ± 47.82	212.75 ± 127.21	134.25 ± 72.97	309.00 ± 162.66
	MPTP	145.50 ± 44.5	434.25 ± 313.19	469.50 ± 659.76	565.25 ± 321.71
	MPTP-NIR II	131.00 ± 27.41	412.25 ± 190.53	260.50 ± 154.68	557.75 ± 224.2
	F	1.53	1.19	0.741	1.42
	P	0.268	0.349	0.504	0.292
CA2	Control	19.00 ± 14.85	33.00 ± 27.35	62.00 ± 32.03	52.00 ± 38.01
	MPTP	25.00 ± 9.56	61.75 ± 32.51	133.25 ± 122.25	86.75 ± 41.48
	MPTP-NIR II	15.25 ± 3.77	44.25 ± 24.47	59.25 ± 46.03	59.50 ± 26.11
	F	0.89	1.05	1.17	1.04
	P	0.444	0.390	0.354	0.391
CA3	Control	78.25 ± 27.32	251.50 ± 65.14	61 ± 39.23	329.75 ± 65.00
	MPTP	105.00 ± 17.63	445.50 ± 73.34	211.00 ± 292.76	550.50 ± 82.40
	MPTP-NIR II	81.75 ± 13.52	367.25 ± 213.84	68.25 ± 21.93	449.00 ± 226.14
	F	2.05	2.07	0.98	2.36
	P	0.185	0.183	0.412	0.150
DG	Control	254.25 ± 92.82	719.00 ± 399.66	200.00 ± 135.28	973.25 ± 420.11
	MPTP	447.25 ± 180.06	1297.00 ± 739.83	887.75 ± 1276.93	1744.25 ± 885.05
	MPTP-NIR II	289.50 ± 113.44	1007.00 ± 832.11	374.00 ± 257.31	1296.50 ± 909.11
	F	2.35	0.72	0.895	1.01
	P	0.151	0.514	0.442	0.403

MPTP, 1-methyl-4-phenyl-1,2,3,6-tetrahydropyridine; NIRII, Near infrared region II; IBA1, ionised calcium-binding adapter molecule 1; GFAP, glial fibrillary acidic protein; APOE, apolipoprotein E.

the MPTP-untreated group, intermediate in the MPTP-NIR-II group, and lowest in the control group (Fig. 3E–H, Table 8). Fig. 4 shows the schematic diagram of cell analysis in the hippocampal CA3 subregion of three groups of rats.

3.3.3. Quantitative analysis of positive cell area in each hippocampal subregion

On the trend chart, the positive cell areas of the CA1, CA2, CA3, and DG subregions were the highest in the MPTP-untreated group, intermediate in the MPTP-treated group, and lowest in the control group (Fig. 3I-L, Table 9).

4. Discussion

PD is the most common degenerative disease of the central nervous system in middle-aged and elderly populations after Alzheimer's disease, affecting 1 % of the global elderly population (≥60 years old) [23]. Cognitive impairment is an essential component of the non-motor symptoms in PD, with an incidence rate six times higher in patients with PD than in healthy individuals, and the risk of occurrence increases with age [24,25]. There are currently no effective treatments for PD. Preparation of experimental models is essential to better understand PD pathogenesis.

MPTP itself is not toxic and is a highly lipophilic organic compound synthesized artificially that can effectively penetrate the blood-brain barrier. In the central nervous system, MPTP selectively catalyzes the formation of an unstable intermediate metabolite, 1-methyl-4-phenyl-2,3-dihydropyridine (MPDP$^+$), via monoamine oxidase B on the outer membrane of astrocyte mitochondria. Subsequently, MPDP$^+$ spontaneously oxidizes to form the stable but toxic 1-methyl-4-phenylpyridinium (MPP$^+$). Owing to its chemical structure, which is similar to that of dopamine, MPP$^+$ can be transported by dopamine transporters from dopaminergic neurons to the cytoplasm. As the concentration gradient gradually increases, this substance interferes with the activity of mitochondrial complex I and blocks the mitochondrial electron transport chain, leading to ATP production disorders, increased oxygen free radical generation, and increased intracellular nitric oxide content, resulting in neuronal degeneration and dopamine death [26–28]. Compared with other models (transgenic models), MPTP-induced PD animal models were the most classic.

The results of the first water maze and rod rotation tests in the present study showed that the escape latency of the model group was significantly prolonged, whereas the drop latency was significantly shortened. Furthermore, residence time in the target quadrant was significantly shortened, and the number of crossing platforms was reduced. These results indicate that MPTP successfully induced learning and cognitive impairment and impaired coordination and balance in rats. Neuropathological and functional neuroimaging studies have supported the role of dopamine and cholinergic deficits in cognitive impairment in PD [29]. The possible mechanisms by which patients with PD may experience the disorders mentioned above include functional abnormalities in the frontal lobe, cingulate gyrus, hippocampus, and thalamus in the default mode network [30–32]; inflammation and oxidative stress in the central nervous system [33,34]; and gray matter atrophy and white matter changes [35–37].

Baik et al. found that PBM improved cognitive function in patients with MCI [38]. The results of this study showed that after NIR-II zone light therapy, the escape latency of the MPTP treatment group was significantly shortened, the target quadrant residence time was significantly prolonged, the number of crossing platforms increased, and the fall latency was significantly prolonged compared with that of the untreated group. The results indicate that NIR-II region illumination significantly improved the learning abilities, cognition, coordination, and balance of MPTP rats. The longitudinal results of this study once again demonstrate the therapeutic effect of NIR-II region illumination. Substantial scientific evidence suggests that PBM can alter neuronal activity and affect survival against damage

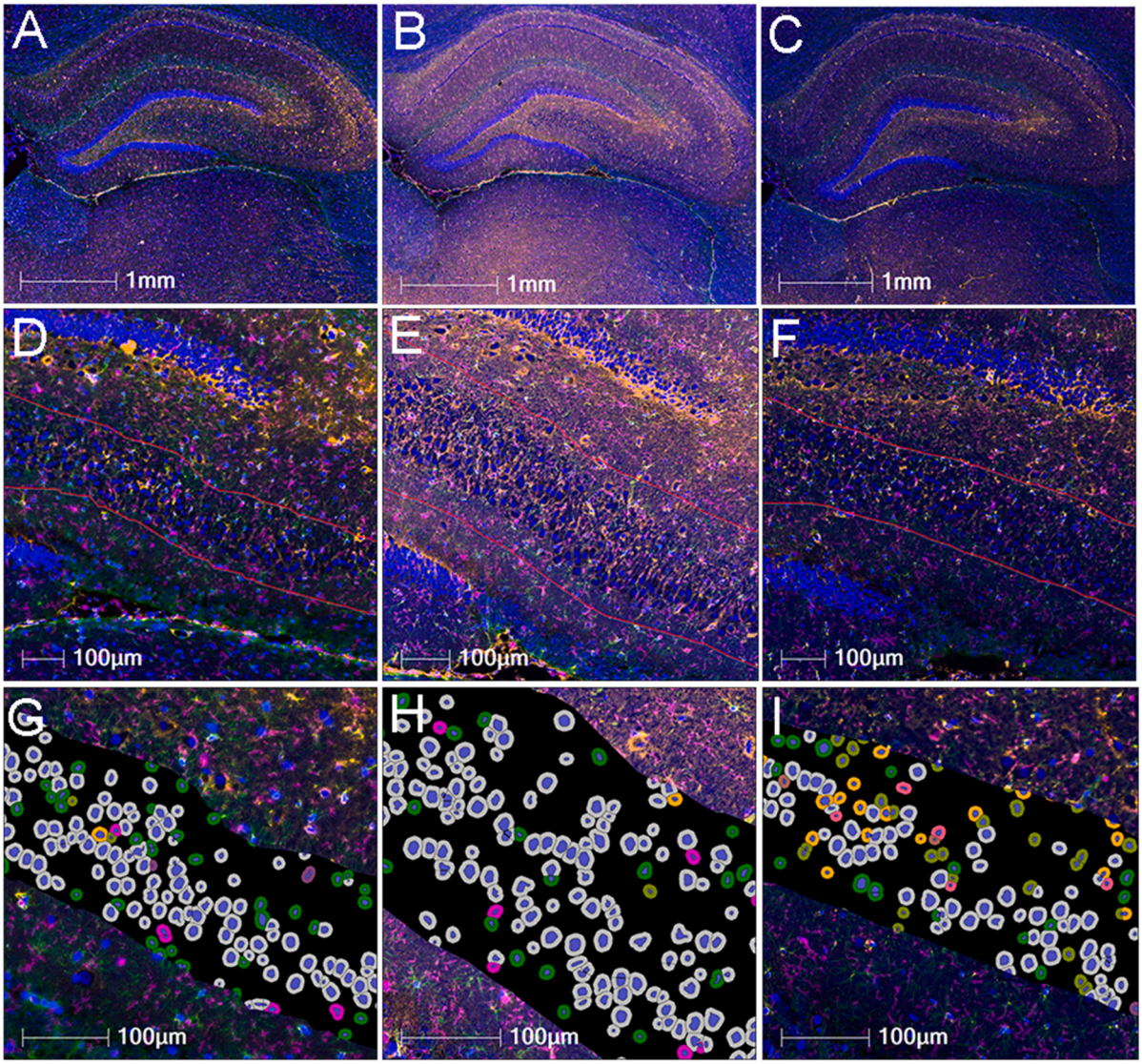

Fig. 4. Schematic diagram of cell analysis in the CA3 subregion of the hippocampus of three groups of rats. Panels A–C are the panoramic images of the hippocampus of the control, MPTP, and MPTP-NIR II groups; Panels D–F are the CA3 subregions of the three groups; Panels G–I are the quantitative analysis patterns of cells of the three groups.

Table 9
Quantitative analysis of positive cell area in the hippocampal subregion of three groups of rats.

Subregions	Control(n = 4)	MPTP(n = 4)	MPTP-NIR II(n = 4)	F	P
CA1	831481 ± 287680.23	1085807.66 ± 102963.41	831481 ± 287680.23	1.77	0.224
CA2	155976.35 ± 38600.11	175074.56 ± 79684.6	161108.34 ± 21202.37	1.41	0.870
CA3	987517.88 ± 137563.21	1115510.58 ± 111429.82	1088951.86 ± 224666.69	0.67	0.536
DG	1189114.8 ± 394467.34	1347410.31 ± 128650.28	1220878.14 ± 183286.37	0.41	0.676

MPTP, 1-methyl-4-phenyl-1,2,3,6-tetrahydropyridine; NIRII, Near infrared region II; IBA1, ionised calcium-binding adapter molecule 1; GFAP, glial fibrillary acidic protein; APOE, apolipoprotein E.

[39]. PBM can also directly affect the cellular metabolism of neurons, downregulate pro-inflammatory markers, and reduce neuroinflammation, thereby reducing neuronal death and improving cell survival rates [40–42].

Neuroinflammation plays a crucial role in the pathogenesis of PD [43–45]. Neuroinflammation is characterized by many activated microglia and astrocytes in the brain region [46,47]. GFAP is a marker of astrocyte activation, IBA1 is a marker of microglial activation, and APOE is primarily produced by astrocytes. Multiple immunohistochemical tests in this study revealed that the number of

GFAP-, IBA1-, and APOE-positive cells in the hippocampal region of the three groups of rat models was the highest in the MPTP-untreated group, intermediate in the MPTP-NIR-II group, and lowest in the control group, regardless of the overall region or subregion. The area of positive cells on the trend chart was also the highest in the MPTP-untreated group, intermediate in the MPTP-NIR-II group, and lowest in the control group. Activated microglia can release pro-inflammatory factors, such as interferon-γ, tumor necrosis factor-α, interleukin-1β, and interleukin-6, to drive progressive damage to dopamine neurons and induce astrocyte activation [48]. Normal astrocytes in the central nervous system can protect neurons by producing antioxidant factors, releasing neurotrophic factors, and clearing toxic neuronal factors. Activated astrocytes release large amounts of inflammatory factors, exacerbating neurotoxicity in the central nervous system. This study's findings demonstrate that NIR-II phototherapy improves learning ability, cognitive impairment, coordination, and balance abilities in rats by downregulating the activation of microglia and astrocytes.

This study had some limitations. First, the MPTP-induced rat model, while commonly used, may not fully replicate all aspects of PD seen in humans. The study was conducted in rats under controlled conditions, limiting the direct translation of the findings to a broader clinical setting or to a different population. Second, this study had a small sample size and only focused on the treatment effects during a specific period. To address potential long-term effects, further research is needed. While the study highlighted correlations between NIR-II phototherapy and improvements in cognitive impairment, elucidating specific underlying mechanisms may require further investigation. Finally, while the study highlighted correlations between NIR-II phototherapy and improvements in cognitive impairment, elucidating specific underlying mechanisms may require further investigation. In summary, MPTP-induced neuroinflammation exists in the hippocampus of PD rats, and NIR-II illumination can improve learning ability, cognitive impairment, and the coordination and balance abilities of rats by inhibiting the activation of microglia and astrocytes.

Data availability statement

Data will be made available on request.

Funding

This work was supported by the National Natural Science Foundation of China (82171908).

Ethics approval statement

This study was approved by the Ethics Committee of Jiangsu Vocational College of Medicine (license no. SYLL-2023-709).

CRediT authorship contribution statement

Jiangong Zhang: Investigation, Data curation. **Qinqin Zhu:** Investigation, Data curation. **Xun Shi:** Investigation, Data curation. **Yang Huang:** Writing – review & editing. **Linlin Yan:** Writing – review & editing. **Guozheng Zhang:** Writing – review & editing. **Lei Pei:** Writing – original draft, Project administration, Formal analysis, Conceptualization. **Jiahuan Liu:** Writing – original draft, Project administration, Formal analysis, Conceptualization. **Xiaowei Han:** Writing – review & editing, Supervision, Resources, Project administration, Funding acquisition. **Xisong Zhu:** Writing – review & editing, Supervision, Resources.

Declaration of competing interest

The authors declare that they have no known competing financial interests or personal relationships that could have appeared to influence the work reported in this paper.

References

[1] Q. Zhang, G.M. Aldridge, N.S. Narayanan, et al., Approach to cognitive impairment in Parkinson's disease, Neurotherapeutics 17 (4) (2020) 1495–1510.
[2] E.R. Wallace, S.C. Segerstrom, C.G. van Horne, et al., Meta-analysis of cognition in Parkinson's disease mild cognitive impairment and dementia progression, Neuropsychol. Rev. 32 (1) (2022) 149–160.
[3] J. Hoogland, J.A. Boel, R.M.A. de Bie, et al., MDS study group "Validation of mild cognitive impairment in Parkinson disease". Mild cognitive impairment as a risk factor for Parkinson's disease dementia, Mov. Disord. 32 (7) (2017) 1056–1065.
[4] Y. Chen, J. Chen, B. Chang, Bioresponsive fluorescent probes active in the second near-infrared window, iRADIOLOGY 1 (1) (2023) 36–60.
[5] A. Bellotti, A review of high-speed optical imaging technology for the analysis of ultrasound contrast agents in an acoustic field, iRADIOLOGY 1 (1) (2023) 78–90.
[6] N. Hong, G.W. Kang, J.O. Park, et al., Photobiomodulation regulates adult neurogenesis in the hippocampus in a status epilepticus animal model, Sci. Rep. 12 (1) (2022) 15246.
[7] S. Shamloo, E. Defensor, P. Ciari, et al., The anti-inflammatory effects of photobiomodulation are mediated by cytokines: evidence from a mouse model of inflammation, Front. Neurosci. 17 (2023) 1150156.
[8] M.F. De Oliveira, D.S. Johnson, T. Demchak, et al., Low-intensity LASER and LED (photobiomodulation therapy) for pain control of the most common musculoskeletal conditions, Eur. J. Phys. Rehabil. Med. 58 (2) (2022) 282–289.
[9] D. Naruseviciute, R. Kubilius, The effect of high-intensity versus low-level laser therapy in the management of plantar fasciitis: randomized participant blind controlled trial, Clin. Rehabil. 34 (8) (2020) 1072–1082.
[10] J. Yang, X. An, Y. Li, et al., Multi-wavelength laser treatments of spider nevi, Laser Med. Sci. 34 (4) (2019) 737–742.
[11] D. Li, W.J. Wu, K. Li, et al., Wavelength optimization for the laser treatment of port wine stains, Laser Med. Sci. 37 (4) (2022) 2165–2178.

[12] L. Santos, S.D. Olmo-Aguado, P.L. Valenzuela, et al., Photobiomodulation in Parkinson's disease: a randomized controlled trial, Brain Stimul. 12 (3) (2019) 810–812.
[13] B. Ahrabi, F.S. Tabatabaei Mirakabad, S. Niknazar, et al., Photobiomodulation therapy and cell therapy improved Parkinson's diseases by neuro-regeneration and tremor inhibition, J. Laser Med. Sci. 13 (2022) e28.
[14] A. Liebert, B. Bicknell, E.L. Laakso, et al., Improvements in clinical signs of Parkinson's disease using photobiomodulation: a prospective proof-of-concept study, BMC Neurol. 21 (1) (2021) 256.
[15] F. Salehpour, J. Mahmoudi, F. Kamari, et al., Brain photobiomodulation therapy: a narrative review, Mol. Neurobiol. 55 (8) (2018) 6601–6636.
[16] M. Hennessy, M.R. Hamblin, Photobiomodulation and the brain: a new paradigm, J. Opt. 19 (1) (2017) 013003.
[17] P. Sun, F. Qu, C. Zhang, et al., NIR-II excitation phototheranostic platform for synergistic photothermal therapy/chemotherapy/chemodynamic therapy of breast cancer bone metastases, Adv Sci (Weinh) 9 (33) (2022) e2204718.
[18] F. Ding, Y. Fan, Y. Sun, et al., Beyond 1000 nm emission wavelength: recent advances in organic and inorganic emitters for deep-tissue molecular imaging, Adv. Healthcare Mater. 8 (14) (2019) e1900260.
[19] V. Jackson-Lewis, S. Przedborski, Protocol for the MPTP mouse model of Parkinson's disease, Nat. Protoc. 2 (1) (2007) 141–151.
[20] M. Mustapha, C.N. Mat Taib, MPTP-induced mouse model of Parkinson's disease: a promising direction of therapeutic strategies, Bosn. J. Basic Med. Sci. 21 (4) (2021) 422–433.
[21] P. Liu, H. Liu, L. Wei, et al., Docetaxel-induced cognitive impairment in rats can be ameliorated by edaravone dexborneol: evidence from the indicators of biological behavior and anisotropic fraction, Front. Neurosci. 17 (2023) 1167425.
[22] S.H. Song, Y.S. Jee, I.G. Ko, et al., Treadmill exercise and wheel exercise improve motor function by suppressing apoptotic neuronal cell death in brain inflammation rats, J Exerc Rehabil 14 (6) (2018) 911–919.
[23] B.L.B. Marino, L.R. de Souza, K.P.A. Sousa, et al., Parkinson's disease: a review from pathophysiology to treatment, Mini Rev. Med. Chem. 20 (9) (2020) 754–767.
[24] O. Hogue, H.H. Fernandez, D.P. Floden, Predicting early cognitive decline in newly-diagnosed Parkinson's patients: a practical model, Parkinsonism Relat. Disorders 56 (2018) 70–75.
[25] E.Sousa C. Severiano, J. Alarcão, I. Pavão Martins, et al., Frequency of dementia in Parkinson's disease: a systematic review and meta-analysis, J. Neurol. Sci. 432 (2022) 120077.
[26] M. Cui, R. Aras, W.V. Christian, et al., The organic cation transporter-3 is a pivotal modulator of neurodegeneration in the nigrostriatal dopaminergic pathway, Proc. Natl. Acad. Sci. U. S. A. 106 (19) (2009) 8043–8048.
[27] S.L. Samodelov, G.A. Kullak-Ublick, Z. Gai, et al., Organic cation transporters in human physiology, pharmacology, and toxicology, Int. J. Mol. Sci. 21 (21) (2020) 7890.
[28] P. Risiglione, L. Leggio, S.A.M. Cubisino, et al., High-resolution respirometry reveals MPP^{+}Mitochondrial toxicity mechanism in a cellular model of Parkinson's disease, Int. J. Mol. Sci. 21 (21) (2020) 7809.
[29] L. Christopher, C. Marras, S. Duff-Canning, et al., Combined insular and striatal dopamine dysfunction are associated with executive deficits in Parkinson's disease with mild cognitive impairment, Brain 137 (Pt 2) (2014) 565–575.
[30] M.G. Li, Y.Y. Chen, Z.Y. Chen, et al., Altered functional connectivity of the marginal division in Parkinson's disease with mild cognitive impairment: a pilot resting-state fMRI study, J. Magn. Reson. Imag. 50 (1) (2019) 183–192.
[31] M.C. Campbell, J.J. Jackson, J.M. Koller, et al., Proteinopathy and longitudinal changes in functional connectivity networks in Parkinson disease, Neurology 94 (7) (2020) e718–e728.
[32] M.G. Li, X.B. Bian, J. Zhang, et al., Aberrant voxel-based degree centrality in Parkinson's disease patients with mild cognitive impairment, Neurosci. Lett. 741 (2021) 135507.
[33] S.Y. Yu, L.J. Zuo, F. Wang, et al., Potential biomarkers relating pathological proteins, neuroinflammatory factors and free radicals in PD patients with cognitive impairment: a cross-sectional study, BMC Neurol. 14 (2014) 113.
[34] A. Anirudhan, G.C. Mattethra, K.J. Alzahrani, et al., Eleven crucial pesticides appear to regulate key genes that link MPTP mechanism to cause Parkinson's disease through the selective degeneration of dopamine neurons, Brain Sci. 13 (7) (2023) 1003.
[35] H. He, L. Liang, T. Tang, et al., Progressive brain changes in Parkinson's disease: a meta-analysis of structural magnetic resonance imaging studies, Brain Res. 1740 (2020) 146847.
[36] A. Lenka, M. Ingalhalikar, A. Shah, et al., Hippocampal subfield atrophy in patients with Parkinson's disease and psychosis, J. Neural. Transm. 125 (9) (2018) 1361–1372.
[37] M. Díez-Cirarda, N. Ibarretxe-Bilbao, J. Peña, et al., Neurorehabilitation in Parkinson's disease: a critical review of cognitive rehabilitation effects on cognition and brain, Neural Plast. 2018 (2018) 2651918.
[38] J.S. Baik, T.Y. Lee, N.G. Kim, et al., Effects of photobiomodulation on changes in cognitive function and regional cerebral blood flow in patients with mild cognitive impairment: a pilot uncontrolled trial, J Alzheimers Dis 83 (4) (2021) 1513–1519.
[39] M.R. Hamblin, Shining light on the head: photobiomodulation for brain disorders, BBA Clin. 6 (2016) 113–124.
[40] C. Dompe, L. Moncrieff, J. Matys, et al., Photobiomodulation-underlying mechanism and clinical applications, J. Clin. Med. 9 (6) (2020) 1724.
[41] M.R. Hamblin, A. Liebert, Photobiomodulation therapy mechanisms beyond cytochrome c oxidase, Photobiomodul Photomed Laser Surg 40 (2) (2022) 75–77.
[42] H. Wu, Q. Liu, C. Meng, et al., Web crawling and mRNA sequencing analyze mechanisms of photobiomodulation, Photobiomodul Photomed Laser Surg 40 (4) (2022) 252–260.
[43] M. Pajares, A. I Rojo, G. Manda, et al., Inflammation in Parkinson's disease: mechanisms and therapeutic implications, Cells 9 (7) (2020) 1687.
[44] C. Marogianni, M. Sokratous, E. Dardiotis, et al., Neurodegeneration and inflammation-an interesting interplay in Parkinson's disease, Int. J. Mol. Sci. 21 (22) (2020) 8421.
[45] A. Jurcau, F.L. Andronie-Cioara, D.C. Nistor-Cseppento, et al., The involvement of neuroinflammation in the onset and progression of Parkinson's disease, Int. J. Mol. Sci. 24 (19) (2023) 14582.
[46] R. Gordon, E.A. Albornoz, D.C. Christie, et al., Inflammasome inhibition prevents α-synuclein pathology and dopaminergic neurodegeneration in mice, Sci. Transl. Med. 10 (465) (2018) eaah4066.
[47] A. Rizor, E. Pajarillo, J. Johnson, et al., Astrocytic oxidative/nitrosative stress contributes to Parkinson's disease pathogenesis: the dual role of reactive astrocytes, Antioxidants 8 (8) (2019) 265.
[48] M.L. Block, J.S. Hong, Microglia and inflammation-mediated neurodegeneration: multiple triggers with a common mechanism, Prog. Neurobiol. 76 (2) (2005) 77–98.